1. Growth of large scale SWNTs via CVD:

To synthesis large scale SWNTs, preparation of catalytic nanoparticles is equally important. We prepared nanoparticles for SWNTs growth via a slightly different method than described in [*Alan M. Cassell et al, "Large Scale CVD Synthesis of Single walled Carbon Nanotubes", J. Phys. Chem. B 1999, 103, 6484*]. In figure 1, we showed step by step synthesis of nanoparticles for SWNTs growth. After the last step we obtained a very fine power of grayish-yellow color.

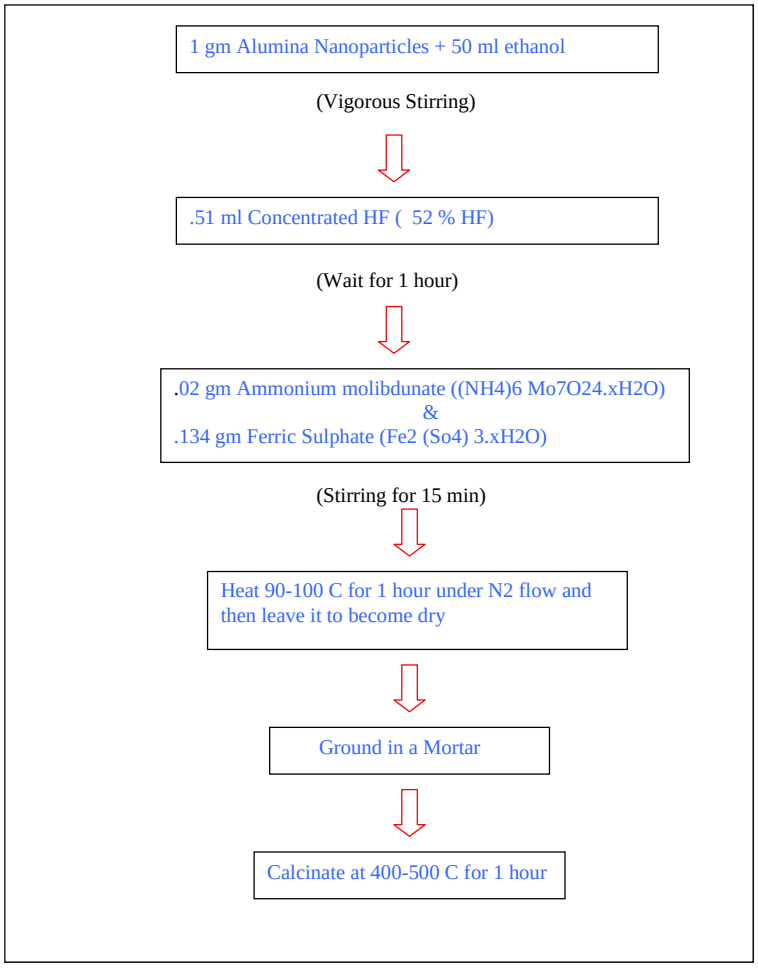

Figure 1: Synthesis of nanoparticles for SWNTs growth.

Growth of SWNTs is done by CVD process using CH_4 as a carrier gas and step by step process is described in figure 2. The process is slightly modified from previously published mehod by Avetik R. Hurutyunyan [*"CVD Synthesis of SWNT under soft conditions" , Nano Letters 2002, vol 2, no 5, 525*]. We had also successfully grown SWNTs in large scales using alcohol (CH_3OH and C_2H_5OH) as well using the same nanoparticles. In both the process (CH_4 and Alcohols), we obtained a fluffy black powder after the growth. TGA analysis showed that after burning the nanotubes in air, 30% (by weight) material left consisting of mainly metal nanoparticles.

Catalyst sample 40-80 mg

⇩

CATALYST REDUCTION STEP:(10 sccm H2 + 90 sccm He) for 10-15 hours at 500 oC

⇩

Change He to 350 sccm Ar and then increase temp by 10 ^{o}C/min up to 850 ^{o}C.

⇩

Flow (350 sccm Ar + 40 sccm CH4 + 10 sccm H2) for 1 hour

⇩

Close the CH4 and H2 valves and Cool the furnace to the room temp with Ar gas flowing

Figure 2: Growth process of large scale SWNTs.

These nanotubes were characterized by Raman, TGA and TEM. In figure 3, we show Raman spectrum of SWNTs prepared by CVD process and using CH4 as a carrier gas. Raman spectrum shows clearly the presence of RBM, D, G and 2D band. Raman technique is a non destructive technique to differentiate between different structures of sp2 carbons. The Shape of G-band (showing G^+ and G^-) and presence of RBM is important for SWNTs. RBM band can be used to estimate the diameter distribution of nanotubes. Calculated diameter of nanotubes (based on RBM) is shown as an inset. Small I_D/I_G established that nanotubes do not have large defect densities.

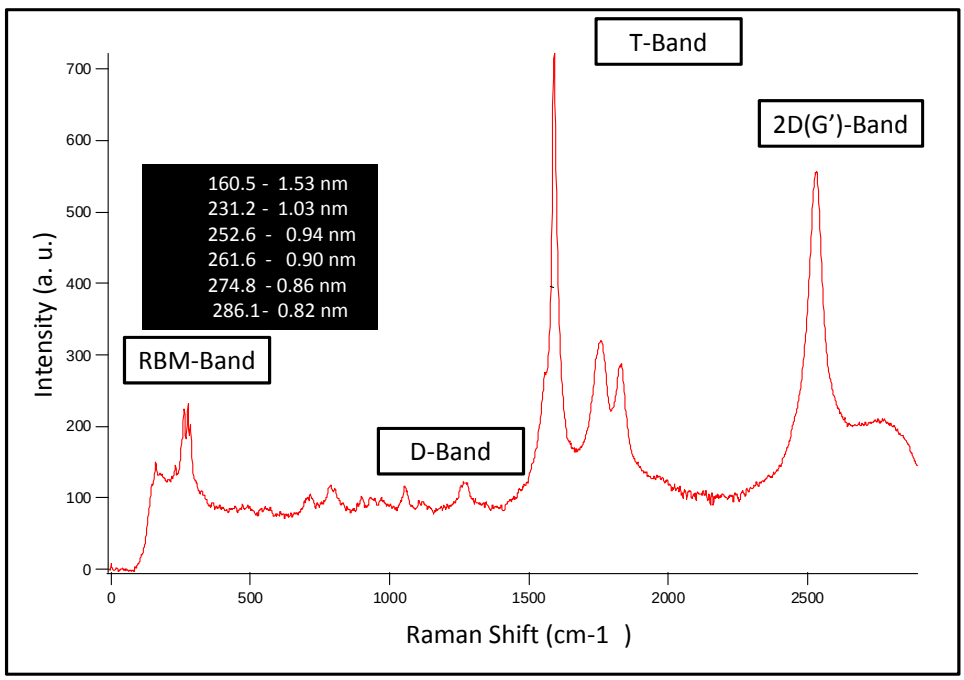

Figure 3: Raman spectrum of SWNTs.

2. Purification and debundling of arc-SWNTs:

SWNTs grown with arc-discharge method have impurities consisting of amorphous carbon, metal nanoparticles, carbon shells etc. To remove all the impurities, our group has developed an effective method. In-short, we first do dry oxidation at ~400 C (temperature and time determine by TGA analysis, shown in figure 4 (c)) for 15 min (~ 120 cc/min dry air) which burns the amorphous carbon and carbon shells covering the metal nanoparticles, we then do acid reflux (HCl and HNO3) to remove the metal contents in the sample.

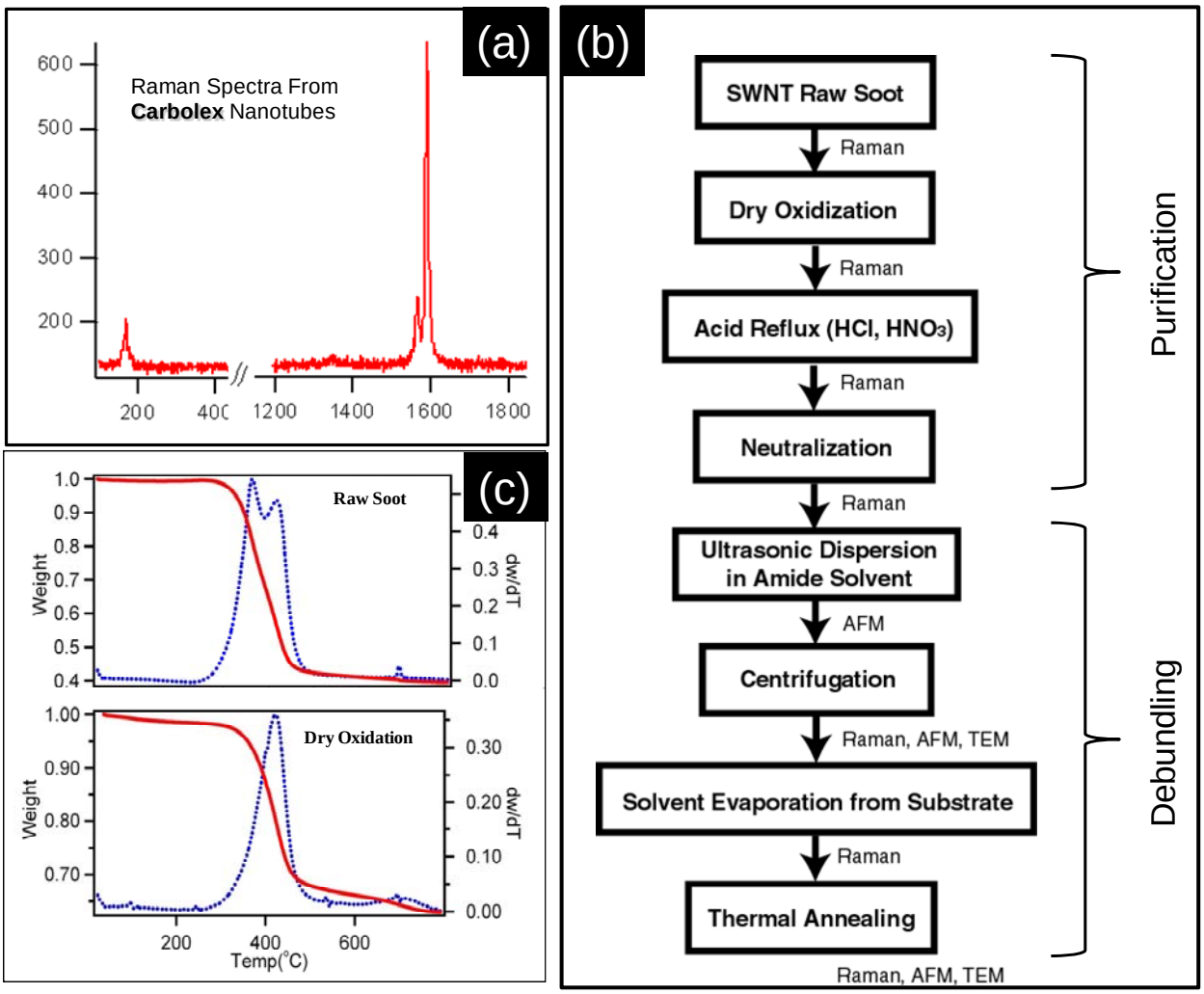

Figure 4: (a) Raman spectra of arc produced nanotubes. (b) A schematic scheme for purification and debundling of nanotubes. (c) TGA of as received material (upper) showing two peaks originating from the amorphous carbon (low temperature peak) and SWNTs (high temperature

peak) and TGA of material after dry oxidation showing the significant decrease in the intensity of peak originating from amorphous carbon.

3. **Growth of isolated SWNTs:**

Growth of isolated SWNTs is important to understand the (n,m) dependence on the physical properties of SWNTs. Preparation of catalytic particles (figure 5) for isolated SWNTs growth is performed by the method first described by *Halfner et al*. The method involves preparing a ferric nitrate solution in IPA and dipping the substrate for 1 min and later washing with hexane. We grown isolated nanotubes at 900 C and used CH_4 as a carrier gas. Nanotubes are grown on Si, SiO_2 and quartz substrate by this method. Figure 5 (right) shows an AFM height image showing the isolated nanotubes grown by this method.

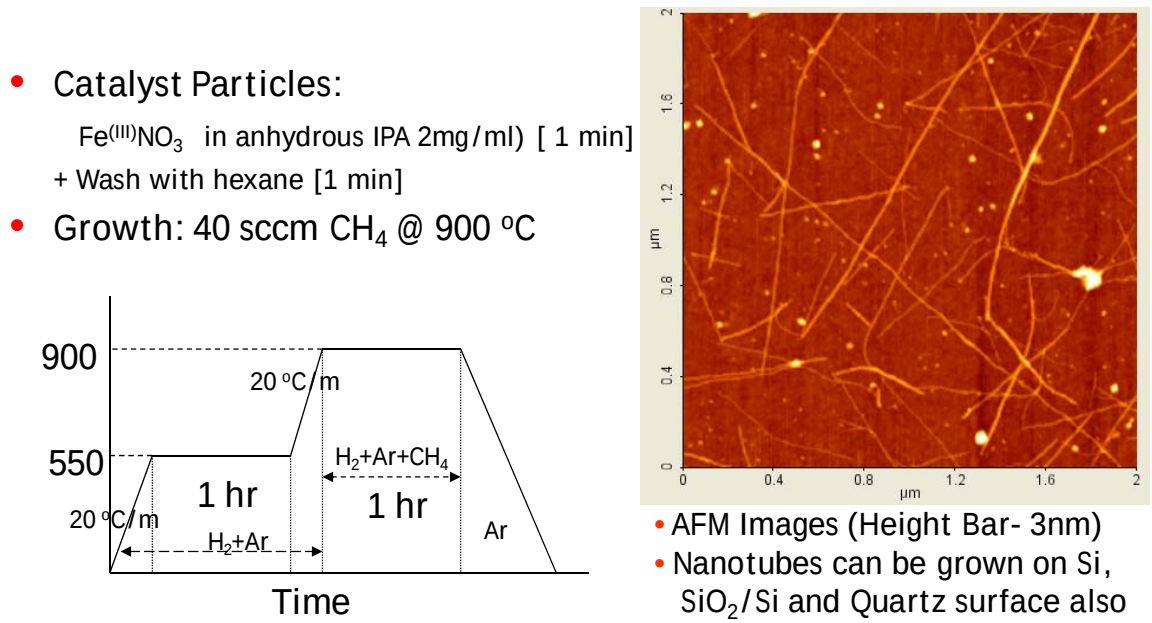

Figure 5: Preparation of catalytic nanoparticles and growth of isolated SWNTs.

Density of nanotubes can be controlled by concentration of ferric nitrate, diameter of nanotubes can be controlled by temperature and length of nanotubes can be control by mixing ethane (C_2H_6) with CH_4 during the growth process. In figure 6 (a), we show the density control of isolated nanotubes per micron^2 area onto the substrate. Left image is 20x20 microns^2 while the right image is 4x4 microns^2. In figure 6(b), we show the diameter control of nanotubes. Left column show nanotubes grown at 1100 C while right column show nanotubes grown at 900 C. At 900 C, we find the diameter distribution to be ~ 0.5-2.0 nm while most probable diameter at 0.8 and 1.2 nm. Diameter distribution of nanotubes is measured with AFM height. At 1100 C, we find nanotubes diameter distribution of ~ 1.0 – 7.0 nm with most probable diameters of ~ 3.0 nm. It was

interesting to see nanotubes as large as 7.0 nm (shown in HRTEM, isolated tube at the bottom image) which is larger diameter ever reported.

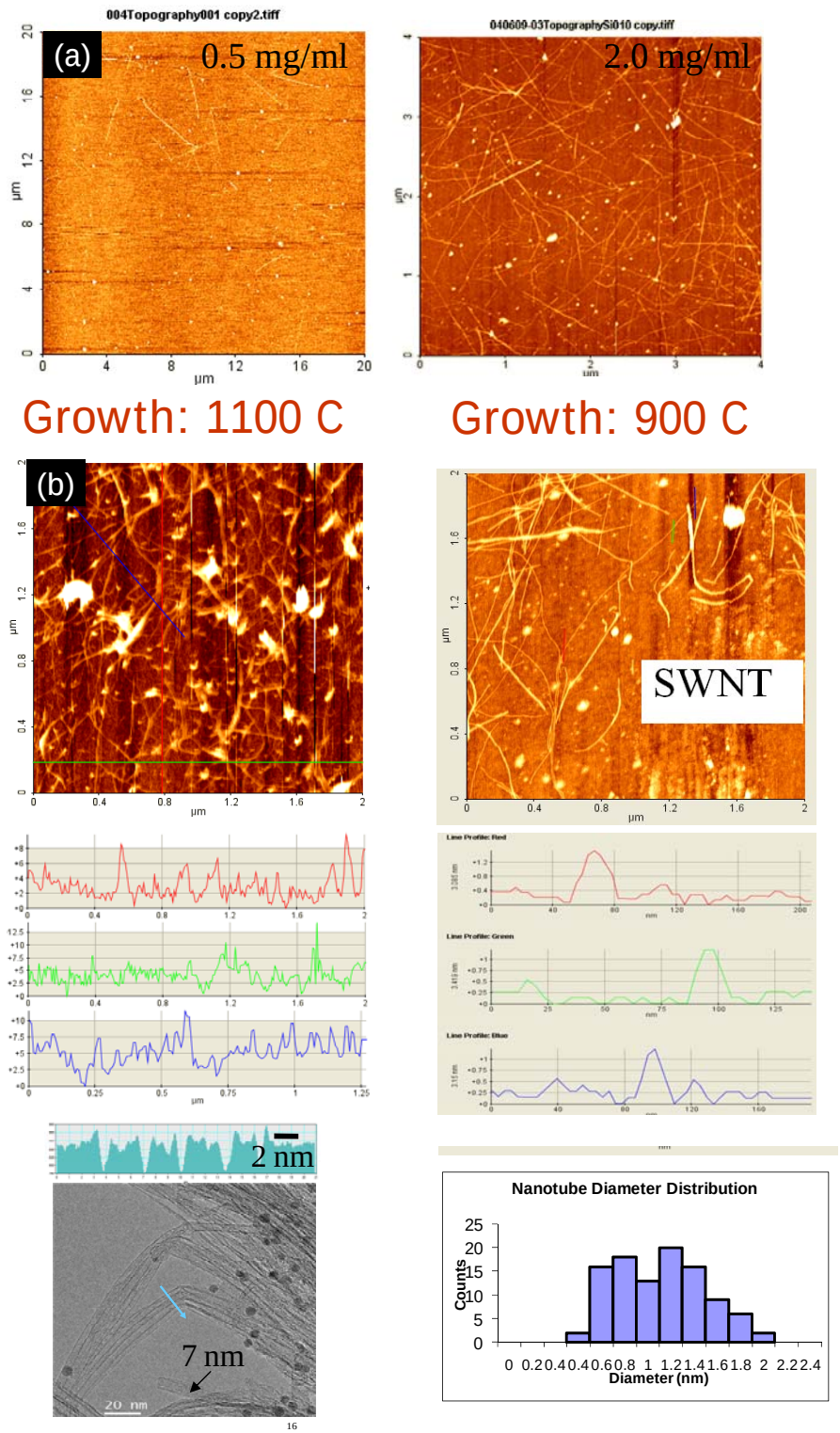

Figure 6. (a) Density control (b) Diameter control

4. SWNTs-FET: Preaparation and Electrical properties:

We studied the effect of nanotube-nanotube junction on the electrical properties of nanotubes prepared by CVD. In figure 7, we show schematic of two kinds of devices studies here: (a) shows a schematic of device where nanotubes are connecting source and drain via percolating network and (b) shows a schematic of device with one or few nanotubes (no junctions) connecting the source and drain. Device shown in fig 7(b) is realized by controlling the density of nanotubes and controlling the spacing between the electrodes. We prepared both of these devices by shadow mask techniques to avoid any chemical exposure (i.e., photoresist etc.)

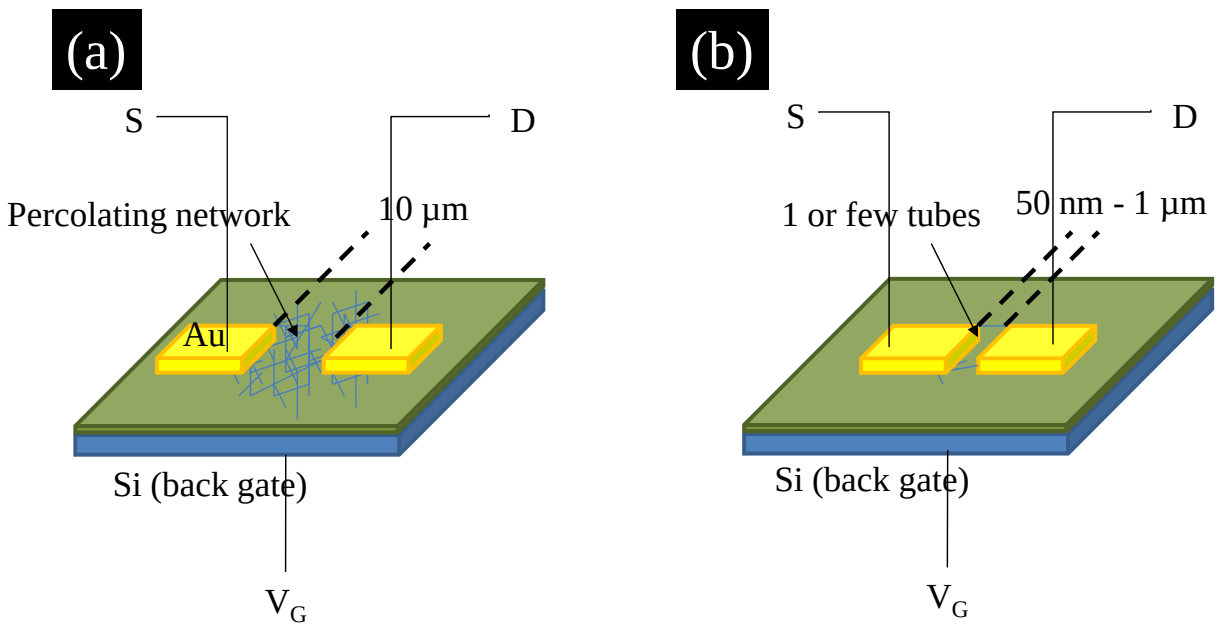

Figure 7. (a) Schematic of FET device prepared by SWNTs percolating network (b) Schematic of FET devices showing one or few SWNTs connecting the S-D electrode. SWNTs are grown by CVD and devices are prepared by shadow mask techniques to avoid any chemical exposure.

4 (a). Device Characteristics (percolating network)

To prepare this kind of devices, we grew high density, short (~ 4 microns in length) SWNTs on Si/SiO_2 substrate. Device is prepared by putting a standard TEM grid (shown in 8(a)) on the substrate and depositing contact pads (source-drain) through hole. Fig 8(b) shows the density of grown nanotubes. We observed few interesting behaviors in these devices: (1) we observed hysteresis in I-V measurement (V_G=0) (fig 8c). This hysteresis behavior can be attributed to the charge trapping [Marty et al *Nano Lett* 3, 1115 (2003)]. At very high current densities (which will depend on the number of nanotubes connecting S-D) we did not

observe very pronounce hysteresis. (2) We observed a presence of conduction peaks at room temperature (RT). These conduction peaks (marked fig 8h, also present in 8g) has previously seen only at low temperature in kinked isolated nanotube [*Dekker et al, Science, Vol. 293, 76 (2001)*] and explained in terms of construction of quantum dot between the kinks. Our results also indicate that the nanotubes cross junction is acting as a quntum dot by sharp bending when one nanotube will lie upon another nanotube [*Nojeh et al Nano Letters , Vol 3, No. 9, 1187-1190 (2003)*]. Experiments on single cross are in progress to verify this.

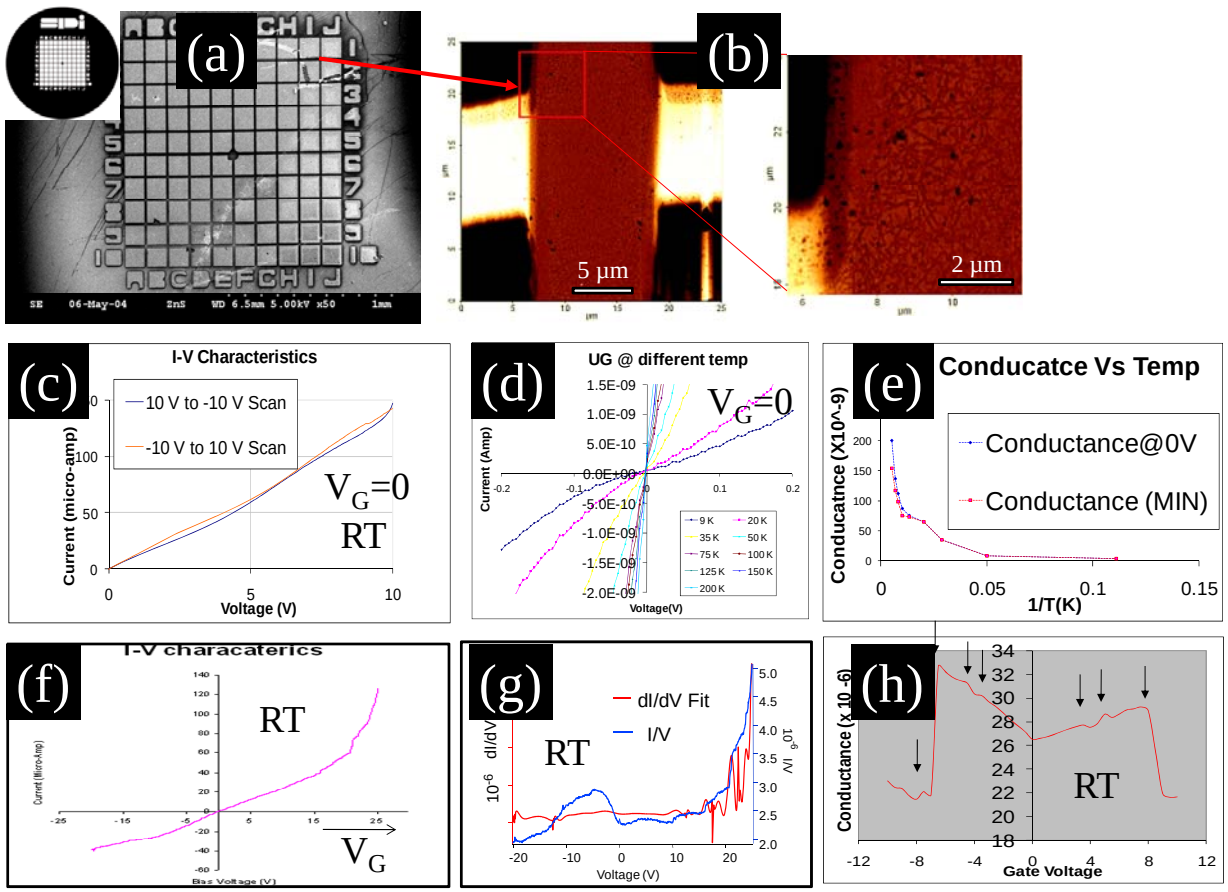

Figure 8 (a) Shadow mask technique (b) AFM of percolating network (c) Hysteresis behavior of device (d) Temperature dependent I-V characteristics (e) Temperature dependent conduction (f) Gate voltage dependence, V_{D-S} ~ 1V (g) Observation of conduction peaks at room temperature for device 1 which are originating from cross junction nanotubes (h) conduction peaks for device 2.

4(b). Device Characteristics (one of few nanotubes)

Devices with only one or few nanotubes connecting the source-drain electrods were prepared by the same way as in section 4(a) but on low density and longer nanotubes. We also controlled the gap between the electrodes by depositing two sources during contact-pads deposition. A schematic is

shown in fig 9(a). fig 9 (b) shows an optical image of the contact pads. We could control the spacing between source and drain from 10's of nanometers to few microns. Unlike high density percolating network devices, we did not see ohmic contact in I-V characteristics (see Fig 9c and 9d). During gate voltage measurements we observed a clear turn on and turn off state similar to reported for isolated nanotubes (fig 9e). Occasionally, we also observed the presence of multimode transport. By this device preparation method, we could prepare 1 or few SWNTs FET devices without exposure to the chemicals.

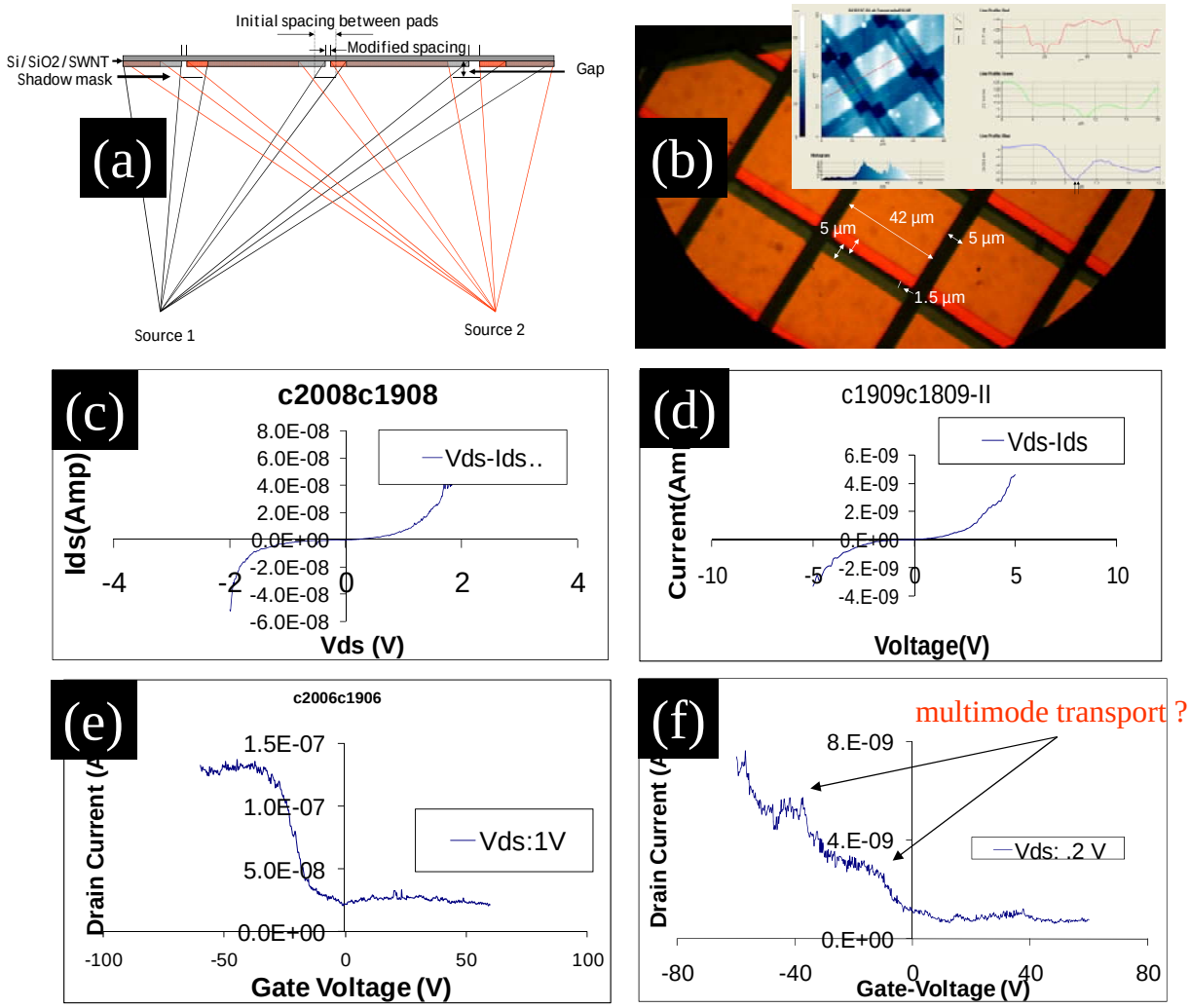

Figure 9. (a) Schematics of method employ to decrease the spacing between electrodes (b) Optical and AFM image of device, (c), (d) I-V characteristics of two devices (e), (f) FET behavior of two devices. (f) Also shows the signature of multimode transport.

5. Boron-doped SWNTs:

In figure 10, we show comparison of Termo Electric Power (TEP) measurements in undoped and B-doped (3% wt) SWNTs mats. Data is collected using home-made apparatus. In figure 10a and 10b, we
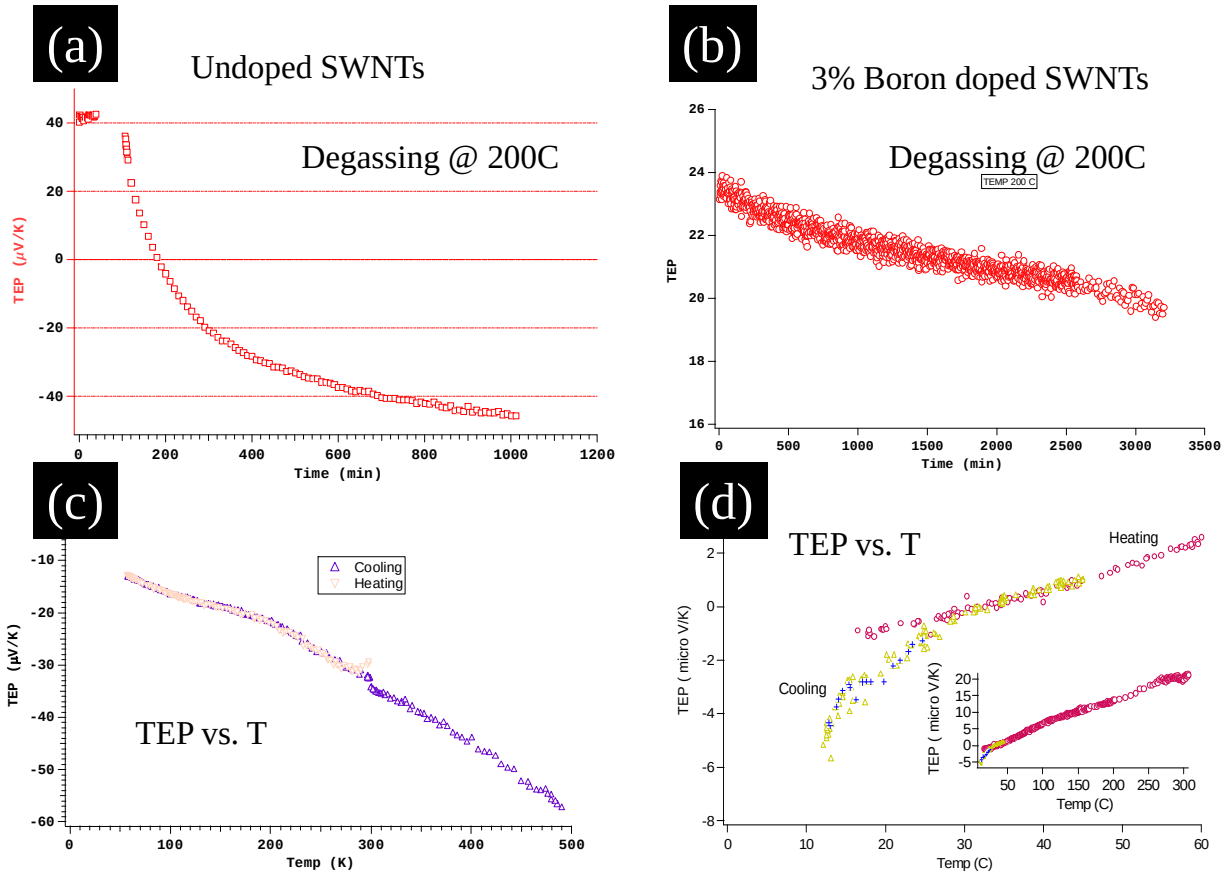
show the change in TEP upon vacuum degassing or undoped nanotubes and B-doped nanotubes. While undoped nanotubes show –ve TEP value after degassing for few hours (after oxygen removal), B-doped nanotubes remain a +ve value even after degassing for few days. In fig 10c, we show the TEP change with temperature after degassing for one day. TEP value goes approaches zero at zero temperature but always remains negative. In the case of B-doped SWNTs, TEP decrease with decreasing temperature but goes from +ve value to –ve value at ~ 30 K. It is very strange behavior as at zero temperature TEP should go back to zero value.